



INFRARED SPECTRAL STUDIES OF TICO SUBSTITUTED Y-TYPE STRONTIUM HEXAFERRITES SYNTHESIZED BY SOL-GEL AUTOCOMBUSTION METHOD

Vijay V. Warhate¹, D. S. Badwaik²

¹Department of Physics, S. N. Mor College, Tumsar, Maharashtra, India

²Department of Physics, Kamla Nehru Mahavidyalaya, Nagpur, Maharashtra, India

ABSTRACT

In the present investigation we synthesized a series of polycrystalline Y-type Sr₂NiMn nano hexa ferrites substituted with TiCo, having generic formula Sr₂NiMnFe₁₂-X(TiCo)X/2O₂₂ (where x = 0, 0.5, 1.0 & 1.5) by novel microwave assisted sol-gel auto combustion route. Structural analysis of the compounds has been studied using X-ray powder diffraction pattern. The prepared compounds are in single Y –type hexagonal phase with the space group R $\bar{3}m$ (no.166). The lattice parameters, experimental density, X-ray density and porosities of compounds were measured from XRD data. It is observed that the lattice parameter “a” is almost remains constant and easy magnetized “c” axis undergoes variation with content of TiCo. The average grain size of the prepared samples measured from Debye Scherer formula is in nanometer range. The powdered samples were sintered at 950 °C for 5 h and characterized by means of DTC, TGA and Fourier transform infrared spectroscopy (FT-IR).

Keywords: Y-type nano hexaferrites, Sol-Gel Auto Combustion, DTC-TGA, FTIR, X-ray Diffraction.

I. INTRODUCTION

Ferrites are useful for microwave applications because they interact with the magnetic component of electromagnetic radiation to produce losses and phase shifts which can be varied with an external magnetic field and which are frequency dependent. These properties make ferrites suitable for applications

to circulators, modulators, isolators, phase shifters, and absorbers, among other applications.

Hexaferrites are classified into six major types depending on their crystal structure and chemical formula. These includes; M-type (BaFe₁₂O₁₉), W-type (BaMe₂Fe₁₆O₂₇), U-type (Ba₂Me₂Fe₂₈O₄₆), X-type (Ba₂Me₂Fe₂₈O₄₆), Y-type (Ba₂Me₂Fe₁₂O₂₂), and Z-type (Ba₃Me₂Fe₃₆O₆₀), where Me represents divalent or trivalent metallic ions [1]. The class of hexagonal ferrites with uniaxial magnetic symmetry contains ferrites whose natural resonant frequency can be chosen by selecting appropriate physical structures (e.g. M, W, X, Y, Z, U) and by making chemical substitutions in the formula (e.g. 1/2 (CoTi), for Fe, or Co for Zn). These modifications allow the greatest microwave activity (phase shift and attenuation) to be placed at the frequency ranges of interest. Examples of such uses are in radar absorbers and isolators. A serious disadvantage of many of the substituted ferrites is that they employ Co ions. Co introduces a strong temperature dependence which shifts the resonant frequency by about 30 MHz/°C near room temperature. In addition, Co has become relatively expensive. Without the use of Co, the known useful substitutions do not fill all of the frequency ranges of interest, subject to other constraints on their properties.

Various ferrites and methods for producing such ferrites have been patented. For example: - in U.S. Pat. No. 4,425,250 (Hibst), U.S. Pat. No. 4,764,300 (Hibst et al), U.S. Pat. No. 4,561,988

(Nagai et al), U.S. Pat. No. 4,781,852 (Kacxur et al) and U.S. Pat. No. 4,786,430 (Mair).

To prepare hexaferrites, several methods have been employed, namely, aerosol pyrolysis, microemulsion, hydrothermal, sonochemical, sol gel, ball milling and coprecipitation technique [16-22].

In present work, Ti^{+4} & Co^{+2} are selected for substituting Fe^{+3} ions in NiMn-Y-type hexaferrite. Moreover, chemical composition of Y-type hexaferrite (i.e. TiCo substituted $Sr_2NiMnFe_{12}O_{22}$) is not reported earlier in the literature.

II. EXPERIMENTAL

A. Synthesis Technique

TiCo substituted Sr_2NiMn -Y hexa ferrite having empirical formula $Sr_2NiMnFe_{12-x}(TiCo)_{x/2}O_{22}$ where $x = 0$ to 1.5 in equal steps of 0.5 were prepared by microwave assisted sol gel combustion method. The starting chemicals used were AR grade strontium nitrate, iron nitrate, zinc nitrate, manganese Nitrate, cobalt nitrate, titanium chloride where used as starting oxidizing material and urea used as reducing agent to supply requisite energy to initiate exothermic reaction amongst oxidants. Stoichiometric amount of starting materials and fuel were dissolved one by one in 30 ml of triple distilled water to prepare a solution, to which urea was added. It is then heated with continuous stirring at 95 °C to form gel.

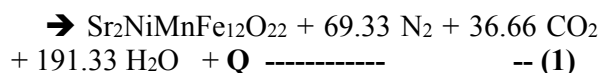
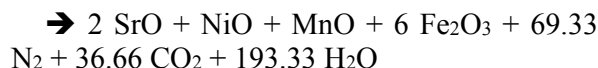
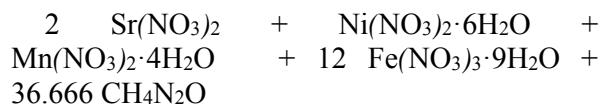
The beaker containing gel was kept in a domestic microwave oven and was irradiated with microwaves having frequency 2.45 GHz. After few minutes dark brown fumes started coming out and gel solution fired into flames and resulted into a foamy dark brown powder. The synthesized compounds were milled in a pestle mortar for about one hour, then calcinated at 950 °C for about five hour in furnace and cooled to room temperature by natural way. The calcinated powder again milled for 1 hour to get fine powder of Y-type nano hexaferrites.

B. Reaction Stoichiometry

To determine the molecules of Urea required, balance the total oxidizing and reducing valence in the mixture, of $Sr_2NiMnFe_{12}O_{22}$ for $x = 0$ leads to : $2(-10) + 1(-10) + 1(-10) + 12(-15) + n(6) = 0$. The total calculated valences of metal nitrates were -220 and +6 for urea (CH_4N_2O).

The stoichiometric redox mixture of the metal nitrates and urea (NO_3^-/Ur), to release the maximum energy for the hexagonal reaction would require that $n = 36.66$ mole for this exothermic redox reaction [8-11].

The complete balanced exothermic redox reaction of the metal nitrates with fuel (urea) can be represented as



In this reaction, the metal nitrates mix with carbon and hydrogen from the urea fuel to form gaseous products like CO_2 , N_2 and water molecule.

C. Sample Characterizations

The structure was determined through the X-ray diffraction (XRD) analysis followed by DTC, TGA and FTIR. XRD patterns were taken using Cu Ka ($\lambda = 1.5406 \text{ \AA}$) radiation at room temperature. The average crystallite size, lattice parameter, experimental density, X-ray density and porosity were calculated using simple formulae.

III. RESULTS AND DISCUSSION

A. Thermal Analysis

The thermal behaviour of the prepared sample was investigated by TGA and DTC. TGA curve "Fig. 1" shown that the weight changes in five regions as 31 °C – 210 °C, 210 °C – 480 °C, 480 °C – 720 °C, 720 °C – 830 °C, 830 °C – 1100 °C are 0.150 % loss, 0.118 % loss, 0.161 % loss, 0.038 % gain and 0.631 % loss of its original weight. The very small loss in weight is observed by removal of absorbed moisture and the exothermic peak at 8400C belongs to the crystallization of Sr-Y ferrite phase formation. [12].

In this research, DTC (differential thermocouple) (Make: PERKIN ELMER,USAA) are used to measure the temperature difference between the hot and the cold junction instead of using two different thermocouples. DTC measure the temperature of the hot block in reference to the cold block.

Hence eliminates the need to use two different TC [13].

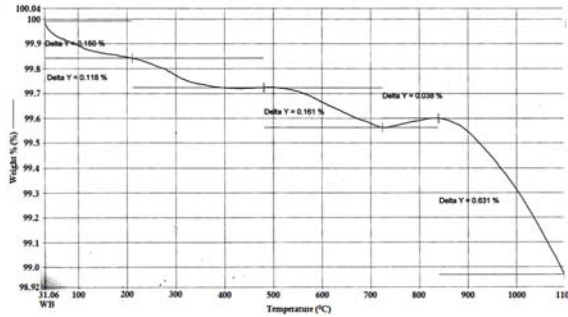


Figure 1: A TGA Curve for Sr₂NiMnFe₁₂O₂₂

The DTC curve “Fig. 2” shows that the alumina relative Seebeck Coefficient, at low temp. SC = +0.2089 μV/K and at high temp. SC = -0.1199 μV/K with transition at 355.34 °C.

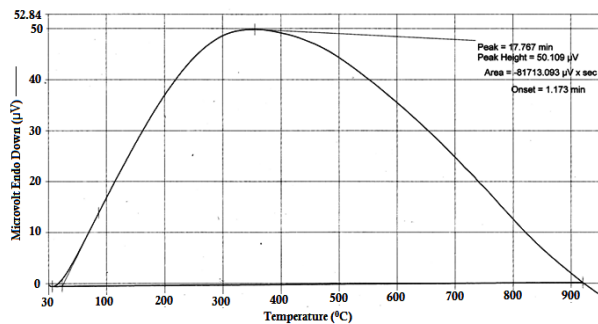


Figure 2: A DTC Curve for Sr₂NiMnFe₁₂O₂₂

B. Structural Analysis

Structural analysis of all TiCo substituted Sr₂NiMn Y –type hexaferrite compounds under investigation were performed by X- ray diffraction pattern shown in Fig. 3. Structural parameters such as crystallite size [14], lattice constants (a and c) along with c/a ratio [15], unit cell volume, X-ray density [16], and porosity [17], were calculated using the following equations.

$$\frac{1}{d^2} = \frac{4}{3} \left(\frac{h^2 + hk + k^2}{a^2} \right) + \frac{l^2}{c^2} \dots\dots\dots --(2)$$

$$V = a^2c \sin 120^0 \dots\dots\dots --(3)$$

$$d_x = \frac{Z.M}{N_a.V} \dots\dots\dots --(4)$$

$$P = \left(1 - \frac{d_b}{d_x} \right) 100 \% \dots\dots\dots --(5)$$

$$d_b = \frac{m}{v_p} \dots\dots\dots --(6)$$

Where, Z is the effective number of molecules per unit cell with a value equal to 3 because in Y-type hexagonal structure unit cell consists of three overlapping of T and S blocks [3(TS)] and oxygen layers [18], M is molecular mass of sample, N_a is Avogadro’s number , V is unit cell volume of specific sample, m and v_p are the mass and volume of the pallet.

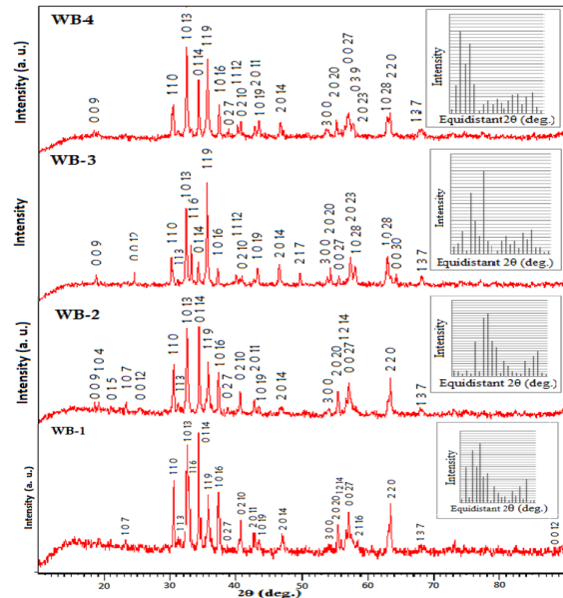


Figure 3: A XRD pattern of Sr₂NiMnFe_{12-x}(TiCo)_{x/2}O₂₂ with x=0, 0.5, 1.0 & 1.5

The crystallographic results of these compounds reveal that, these are Y–type hexagonal ferrites and most of the peaks matched with standard XRD pattern of Y-type hexa ferrite. All the compounds belong to the R3̄m(no.166) space group. It is observed that the lattice parameter “a” is almost remains constant and easy magnetized “c” axis undergoes variation with content of TiCo. This variation in the lattice parameter “c” can be explained on the basis of the ionic radii. The ionic radii of the Ti+4 ion is (0.74 Å) and Co+2 ion is (0.72 Å). Due to the difference in the ionic radii of Ti+4 and Co2+ than that of Fe3+ (0.64 Å), the variation in lattice parameters with TiCo substitution is expected. It is also shown that the values of the lattice parameters are in satisfactory agreement with the published results for Y-type hexagonal ferrites [19], where a=5.86Å and c=42.47Å. The value of x-ray density for all compounds are compatible with that reported in the literature i.e. 5.2 gm/cm³. [20] However, the experimental

density d_b values were found to be much smaller than the X-ray density d_x , indicating that prepared compounds are highly porous materials.

Table - II shows a decrease in the bulk density and a corresponding increase in porosity P with increase in content of Ti, Co ions. This behavior may be attributed to the fact that the introduction of Ti, Co ions in hexaferrite affects the grain size development during sintering. The XRD pattern is also used to calculate the grain size of the prepared compounds using Scherar's formula [21] from most intense peak as given below.

$$D = (0.9\lambda) / (\beta \cos\theta) \dots \dots (7)$$

where λ is the wavelength of radiation used, β is full width at half maxima of strongest peak of pattern, θ is the diffraction angle, d is the distance between lattice planes, hkl and a & c are miller indices and the lattice parameters, respectively. The crystallite size calculated is found to be in range of 49 nm to 71 nm.

TABLE I
STRUCTURAL PARAMETERS OF $Sr_2NiMnFe_{12-x}(TiCo)_x/2O_{22}$

Compound	Lattice Parameters		Ratio c/a	Cell Volume (Å) ³
	a (Å)	c (Å)		
x = 0.0	5.8474	42.6318	7.2907	1262.38
x = 0.5	5.8500	42.5765	7.2780	1261.88
x = 1.0	5.8274	42.4137	7.2783	1247.36
x = 1.5	5.8478	42.5060	7.2687	1258.84

TABLE II
STRUCTURAL PARAMETERS OF $Sr_2NiMnFe_{12-x}(TiCo)_x/2O_{22}$

Compound	d_b gm/cm ³	d_x gm/cm ³	P %	Grain Size (nm)
x = 0.0	3.8477	5.1735	25.63	61.85
x = 0.5	3.6259	5.1707	29.88	61.55
x = 1.0	3.4913	5.2260	33.19	70.70
x = 1.5	3.4773	5.1735	32.79	49.47

C. FTIR Analysis

The application of infrared spectroscopy to the identification of inorganic compounds is widely used [22]. In the present research, infrared spectra of inorganic compounds in the solid phase in mid infra red region 4000-400cm⁻¹ are presented in "Fig. 4". All compounds are (powdered) crystalline solids in which the crystallographic unit cell contains several polyatomic ions. The internal modes of vibration of the polyatomic group generally occur in the region 4000-400cm⁻¹. When standard spectra are available, a compound such as KN₃ can easily be distinguished from NaN₃ or Ca(N₃)₂, but in the absence of standard spectra, specific identification of a cation-anion pair is usually not possible by infrared spectroscopy [23].

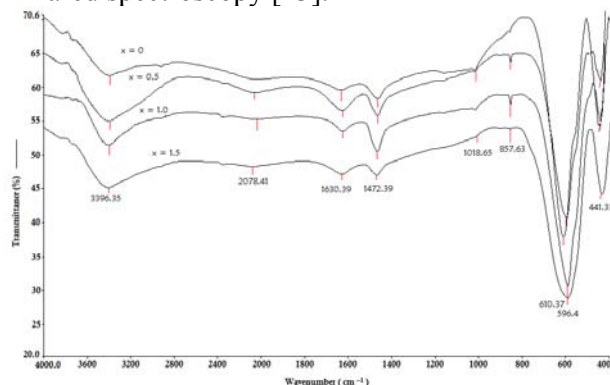


Figure 4: Infrared Spectra of $Sr_2NiMnFe_{12-x}(TiCo)_x/2O_{22}$

Comparison of standard infrared spectra [24-25] of starting compounds with prepared compound is given in Table III and IV. It is seen in "Fig. 4" that for all samples, there exist two absorption bands in the range 442 cm⁻¹ and 600 cm⁻¹, which corresponds to the asymmetric stretching vibrations of metal cations (M-O) at octahedral and tetrahedral lattice sites respectively [26]. The low frequency band appearing around 442 cm⁻¹(ν_2), and high frequency band around 600 cm⁻¹(ν_1) are common representation of spinel ferrite structure.

TABLE III
COMPARISON WITH STANDARD CHARACTERISTIC FREQUENCIES

Fe(NO ₃) ₂ 9H ₂ O		Co(NO ₃) ₂ 6H ₂ O	
Freq. cm ⁻¹	Intensity	Freq. cm ⁻¹	Intensity
835	W	807	VW
1361	VS	836	W

1615	M	1372	VS
1785	VW	1640	M
2440	VW	2410	S
3230	S	3230	M

TABLE IV
COMPARISON WITH STANDARD CHARACTERISTIC
FREQUENCIES

Sr(NO ₃) ₂		Sr ₂ NiMnFe ₁₂ O ₂₂	
Freq. cm ⁻¹	Intensity	Freq. cm ⁻¹	Intensity
--	--	441	VS
737	S	594-610	VS
815	S	857	W
1382	VS	1018	VW
1441	VS	1472	S
1795	VW	1630	S
2420	VW	2078	VW
3450	W	3396	S

*S-strong, W-weak and M-medium intensity.

In hexagonal structure these bands are attributed to cations vibrations present in the spinel block of Y-ferrite [27]. It has been noticed that with increase in TiCo concentration, ν_1 shift towards higher wavenumber side. This gradual shift of band can be associated to the replacement of cation with larger ionic radius, which resultantly affects the cation-anion stretching at octahedral and tetrahedral lattice sites.

IV. CONCLUSION

A series of polycrystalline Sr₂NiMn Y-type nano hexaferrites substituted with TiCo having generic formula Sr₂NiMnFe_{12-x}(TiCo)_{x/2}O₂₂ were successfully prepared by novel microwave assisted sol-gel auto combustion method. The Xray diffraction pattern and FTIR confirmed the formation of single Y-type hexaferrite phase in all prepared compounds. The crystallite size is found to be in range of **49** nm to **71** nm. The experimental density values were found to be much smaller than the X-ray density, indicating that prepared compounds are highly porous materials.

The DTC curve shows that the alumina relative Seebeck Coefficient, at low temp. SC = +0.2089 μ V/K and at high temp. SC = -0.1199 μ V/K with transition at 355.34 °C.

V. REFERENCES

- [1] S. Shen, Y. Chai, Y. Sun, Sci. Rep. 5 (2015) 8254-8262
- [2] T.G. Carreno, M.P. Morales, C.J. Serna, Mater. Lett. 43 (2000) 97-101.
- [3] J. Fang, J. Wang, L. Gan, S. Ng, J. Ding, X. Liu, J.Am. ceram. Soc. 83 (2000) 1049-1055.
- [4] D. Primc, D. Makovec, D. Lisjak, M. Drofenik, Nanotechnology 20 (2009) 315605.
- [5] K.V.P.M. Shafi, A. Gedanken, Nanostr. Mater. 12 (1999) 29-34.
- [6] S.H. Mahmood, F.S. Jaradat, A.F. Lehlooh, A. Hammoudeh, Ceram. Intern. 40 (2014) 5231-5236.
- [7] [21] S.H. Mahmood, A.N. Aloqaily, Y. Maswadeh, Solid State Phenom. 232 (2015) 65-92.
- [8] W. Eerenstein, N.D. Mathur, J.F. Scott, Nature 442 (2006) 759-765.
- [9] N.A. Spaldin, S.W. Cheong, R. Ramesh, Phys. Today 63 (2010) 33-38.
- [10] Barkat Ul-ain, S. Ahmed, M. Anis ur Rehman, Y. Huangb, C.A. Randall, New J. Chem. 37 (2013) 2768-2771.
- [11] Z. Haijun, Y. Xi, Z. Liangying, J. Eur. Ceram. Soc. 22 (2002) 835-840.
- [12] Frank J. Blatt, et al. Thermoelectric Power of Metals. Plenum Press, New York and London. 1976.
- [13] Robin E. Bentley. Theory and Practice of Thermoelectric Thermometry. Vol. 3 Spinger-Verlag, Singapore. 1998.
- [14] B.D. Cullity, Elements of X-ray Diffraction, Indiana, Notre Dame, 1977, pp. 90-91.
- [15] U. Khan, N. Adeela, K. Javed, S. Riaz, H. Ali, M. Iqbal, X.F. Han, S. Naseem, J. Nanoparticles Res. 17 (2015) 429-437.
- [16] A. Elahi, M. Ahmad, I. Ali, M.U. Ranan, Ceram. Int. 39 (2013) 983-990.
- [17] M.J. Iqbal, M.N. Ashiq, P.H. Gomez, J.M. Munoz, J. Alloys Compd. 500 (2010) 113-116.
- [18] Y. Salunkhe, D. Kulkarni, J. Magn. Mater. 279 (2004) 64-68.
- [19] Badwaik V., Badwaik D., Nanoti V., Rewatkar K., International Jour. of Knowledge Engineering, **2012**, 3, 1, 58-60.

- [20] Safaan S. A., Abo El Ata A.M., El Messeery M.S., J. Magn. Magn. Mater. **2007**, 302, 362- 367.
- [21] Lee, J. D. (Eds.); Concise Inorganic Chemistry; Wiley: UK, **1996**.
- [22] G. Herzbag, 'Molecular spectra and Molecular structure I spectra of Diatomic Molecules', second edition, D. Van Nostrand Co. (1950) p458.
- [23] E. Nakamoto, "Infrared Spectra of Inorganic and Coordination Compounds," p. 87. Wiley, New York, 1963.
- [24] Infrared and Raman Spectroscopy – Methods and application by Bernhard Schrader, VCH pub. USA, 1995
- [25] L. J. Bellamy, "The Infrared Spectra of Complex Molecules." Wiley, New York, 1958.
- [26] N. Adeela, K. Maaz, U. Khan, M. Iqbal, S. Riaz, S. Naseem, Nanomaterials 6 (2016) 73.
- [27] Binu P Jacob, Smitha Thankachan, Sheena Xavier and Mohammed E M, *Phys Scripta.*, 2011, **84**, 045702.